

Assessment of compliance with RF EMF exposure limits: Approximate methods for radio base station products utilizing array antennas with beam-forming capabilities

E. Degirmenci, B. Thors, and C. Törnevik, *Member, IEEE*

Abstract— The importance of antenna arrays with beam-forming capability is expected to increase in future mobile communication systems with the ongoing development of new radio access technologies involving higher frequency bands and massive MIMO concepts. In this paper, various approximate methods for radio frequency electromagnetic field compliance assessments of radio base station products utilizing these antenna arrays are investigated with the focus on front compliance distances. For electrically large arrays, the results show that accurate compliance boundary dimensions may be obtained using a field-combining procedure of assessment results for a centrally placed element. For smaller arrays, an overall improvement in accuracy is possible by complementing the center element solution with results for a handful of selected edge and corner elements to better characterize the array behavior. Compared with a general and straight-forward approach based on field combining of embedded assessment results for each element, the approximate methods allow for significant reductions of the total assessment time.

Index Terms— RF EMF compliance, Radio access networks, Base stations, 5G mobile communication, Antenna arrays, MIMO, Beam steering

I. INTRODUCTION

BYOND 2020 wireless communication systems will need to support traffic volumes more than 1,000 times larger than today and achieve peak data rates up to ten gigabits per second [1]. For the fifth generation (5G) radio access technologies, utilization of beam-forming and massive multiple-input-multiple-output (MIMO) concepts are anticipated to play an important role to meet the expected demands on capacity and reliability [2, 3].

In addition to the existing cellular bands, 5G systems will also involve higher frequency bands, offering both new possibilities and challenges. For instance, the increase in

available spectrum at higher frequencies not only opens up the possibility of wider transmission bandwidths, but also enables the deployment of massive antenna configurations consisting of a very large number of antenna elements with small to modest physical footprint due to the reduced wavelength [4]. One of the main advantages of utilizing large antenna arrays is the possibility of electronic beam steering in elevation and azimuth to focus energy towards the intended user equipment as a tool to improve the link budget.

All radio base station (RBS) products emitting radio-frequency (RF) electromagnetic fields (EMF) need to be designed and tested to comply with relevant regulatory requirements on human exposure. The aim of these product compliance tests is to determine compliance boundaries outside of which the RF EMF exposure is below the relevant limits. The most widely adopted exposure guidelines have been specified by the International Commission on Non-Ionizing Radiation Protection (ICNIRP) [5]. Restrictions on exposure to EMF based directly on established health effects are termed basic restrictions. For practical exposure assessments another set of limits, denoted reference levels, are specified. Compliance with the reference levels should ensure compliance with the relevant basic restriction [5].

In the frequency range between 10 MHz and 10 GHz, the ICNIRP basic restrictions are specified in terms of specific absorption rate (SAR). SAR is a measure of the rate of absorbed energy inside the human body and requires either expensive measurement systems or advanced numerical simulations. In contrast, the corresponding reference levels, given in terms of free space electric and magnetic field strengths, allow for much simpler assessments. At higher frequencies, the power absorption becomes increasingly superficial and from 10 GHz to 300 GHz the ICNIRP basic restrictions are given in terms of free space power density.

Product compliance assessment methods fulfilling the requirements of the European regulations are described in the European standard CENELEC EN 50383 [6]. The assessments are to be conducted using either measurements or calculations for free space conditions without considering the effects of scatterers and/or ambient sources.

For RF exposure assessments of multi-port antennas enabling MIMO transmissions, the combined exposure from

E. Degirmenci, B. Thors, and C. Törnevik are with Ericsson Research, Ericsson AB in Sweden (e-mail: elif.degirmenci@ericsson.com; bjorn.thors@ericsson.com; christer.tornevik@ericsson.com).

all ports needs to be considered. Depending on the multi-antenna system used, the electromagnetic fields may be either correlated or uncorrelated. Guidance on how to combine exposures from multiple electromagnetic (EM) sources in terms of SAR or power density is given in [7].

RF exposure compliance methodologies for MIMO enabled base station applications have been reported in [8]. Different field combining methods were considered for a scenario with two vertically polarized base station antennas horizontally separated by 10 wavelengths. Due to the relatively large spacing between the antennas, the mutual coupling is weak and of minor importance in the analysis. In [9], numerical EMF exposure assessments were performed for a multi-column base station array antenna with densely spaced elements. The array antenna, intended for beam-forming applications, experience quite strong mutual coupling between the antenna ports. Various field combining methods were investigated and a good agreement with reference measurements was observed. It was shown that accurate and efficient EMF compliance assessments can be conducted by employing an (i) embedded element approach [10, 11], where each element is assessed sequentially with all the other elements terminated in matched loads, followed by a (ii) conservative field combining procedure [9]. This basic approach is rigorous and is used as a reference solution in this work. Long Term Evolution Advanced (LTE - Release 10+) allows for up to 8 antenna ports at the base station [12]. Thus, following the approach in [9], RF EMF compliance assessments of existing mobile communication MIMO systems require up to 8 embedded element simulations. Future radio access technologies will most likely make use of much larger antenna arrays with up to several hundreds of antenna elements, for which this procedure becomes very costly in terms of assessment time and resources.

In this paper, numerical RF EMF exposure assessments of various sized array configurations have been investigated with the aim of finding an accurate and efficient compliance assessment procedure for RBS products utilizing large array antennas with beam-forming capability. Front compliance distances using different approximate methods based on the characteristics of a central element or a few elements essential for describing the array behavior have been investigated and compared with the full embedded element solution. Although the data for the analysis are obtained using numerical simulations, the methods proposed are general in nature and may be applied also for measurement-based compliance assessments.

The rest of the paper is organized as follows. The approximate methods investigated are described Section II and the results are presented in Section III. This is followed by a discussion in Section IV, and finally, some conclusions are presented in Section V.

II. METHOD

A. Compliance Boundary

A compliance boundary is described as a surface outside of which the RF exposure is below the exposure limits. The compliance boundary may be determined with respect to either the basic restrictions or, as in this paper, with respect to

the reference levels. Depending on the complexity of the antenna, the surrounding field distribution, and hence the most accurate compliance boundary, may be quite complex. For practical reasons, a conservative approach is often used where the compliance boundary is specified in terms of a simpler geometrical object; such as a rectangular box characterized by its width, height, and the distances behind and in front of the antenna [6]. The compliance distance is the distance in a certain direction from the antenna to the compliance boundary. The largest exposure is normally obtained in the front direction.

For beam-forming arrays, a careful choice of the antenna element excitations is used to focus the transmitted energy in the desired direction(s). Subject to applications, and depending on the radio conditions, the antenna element excitations are likely to vary over a time frame much shorter than the averaging time prescribed for RF exposure assessments, which normally is in the order of minutes [5]. In this case, combining electromagnetic field strengths as a sum of true vector fields may not be possible. Therefore, exposure from multiple electromagnetic sources is normally assessed for a worst-case situation where the exposure is maximized in every evaluation point according to Eq. (2), see also [9]. Although the resulting field distribution is not possible to realize with any set of antenna element excitations, the approach is justified by the objective to determine a compliance boundary which is conservative for all possible excitations.

B. Numerical Simulations

Numerical simulations in order to assess EMF exposure from various sized array antennas were carried out at 2 GHz using the commercial electromagnetic solver FEKO (Altair, Stellenbosch, South Africa), which is an integral equation solver based on the Method of Moments (MoM) [13].

Square-sized arrays, ranging from 3x3 to 15x15 elements, were investigated using simplified antenna models. The antennas consisted of ground-plane-backed arrays of 45° slanted dipole elements represented by straight wires fed with voltage sources at the center of each element, see Fig. 2. Due to the polarization orthogonality, compliance boundaries for X-polarized dipole arrays can easily be obtained from simulations of the 45° slanted dipole array using the approach in [9].

The distance between the reflector and the dipoles was $\lambda/4$, where $\lambda \approx 0.15$ m denotes the free space wavelength. Separation distance between the dipole elements of $\lambda/2$ was investigated to facilitate beam steering without the introduction of grating lobes [14], and each element was surrounded by metallic walls with a height of $\lambda/5$. In the simulations, all metallic structures were represented by either triangular patches with a maximum edge length of $\lambda/8$ or wire segments with the maximum length of $\lambda/10$.

The electric and magnetic field strength levels were assessed on a uniform grid of discrete points in a 3D volume of appropriate size surrounding the antenna. The step size between the field samples was 0.1m and the compliance boundaries were determined from the full 3D data set by

comparing the obtained peak field strength results with the reference levels according to the following procedure:

The total exposure ratio (ER), expressed in terms of electric and magnetic fields at the assessment point \mathbf{r} in the vicinity of a multiport antenna is first determined as

$$ER(\mathbf{r}) = \max\left(\frac{E_{rms}(\mathbf{r})^2}{E_{lim}(f)^2}, \frac{H_{rms}(\mathbf{r})^2}{H_{lim}(f)^2}\right) \quad (1)$$

where E_{rms} and H_{rms} correspond to the root-mean-squared (rms) electric and magnetic fields obtained using either the Reference solution or the Approximate solutions described in Section II.C and II.D, respectively. $E_{lim}(f)$ and $H_{lim}(f)$ denote the corresponding reference levels (exposure limits) for the electric and magnetic fields at frequency f , respectively.

Finally, the box-shaped compliance boundary is obtained as the smallest box which circumscribes the iso-surface for which $ER(\mathbf{r}) = 1$.

C. Reference Solution

A key point in this investigation is that each element needs to be fed individually to allow beam-forming in both elevation and azimuth. Therefore, a conservative compliance boundary should be determined for all possible antenna element excitations with the side condition that overly-conservative assumptions are avoided. Furthermore, due to the small inter-element spacing for these arrays it is important to consider the effect of mutual coupling for accurate results. To satisfy both these requirements an embedded element approach may be used in combination with a conservative field combining technique. This method has been verified with measurements [9] and is used as a reference solution in this work. Thus, for an array with $N \times N$ elements, field strengths results of N^2 separate embedded element assessments are required to determine the reference solution.

Once the field strengths are obtained for each antenna element, the correlated field contributions are combined using the Magnitude method [7] where the combined electric field strengths can be written as

$$E_{rms}(\mathbf{r}) \leq \sum_{n=1}^{N^2} |w_n| |E_n(\mathbf{r})|_{rms} \quad (2)$$

where w_n and E_n denote the complex excitation coefficients and the electric field associated with port n , respectively. N^2 denotes the total number of antenna ports. In this work, a uniform amplitude excitation is assumed. The relation in Eq. (2) is in terms of the electric field strength but apply also for the magnetic field.

D. Approximate Solutions

As noted earlier, the embedded element approach used as reference in this work becomes unpractical when large array antennas are considered since separate assessments are required for each antenna port. Moreover, for assessments based on numerical simulations the simulation time per element also increases with the physical size of the array. An approximate assessment method is therefore needed with an overall objective to produce accurate compliance boundaries in an efficient manner.

In this context it is key to first find characteristics that describe the behavior of large arrays. A fundamental property of array antennas is that the antenna elements couple to each other. This coupling is, in general, strongest between adjacent elements. Elements located on the edge of the array will therefore sense a somewhat different environment compared with elements located in the center of the array.

As an example, impedance characteristics for a uniformly excited 10×10 array are shown in Fig. 1 as function of the element position in the array. The element numbers are given row-by-row starting with the first element in the lower left corner and ending with the last element located in the upper right corner. Consequently, dipole numbers 1, 10, 91 and 100 correspond to the corner elements of the 10×10 array. Note that no attempts were made to match the elements to specific source impedances. As shown in Fig. 1, the real parts of the impedances are relatively stable as function of element position while the imaginary parts display a more location dependent behavior. In this example, elements with a reactance of approximately 40 ohms are located in the central part of the array whereas elements with reactances of approximately 60 and 80 ohms correspond to edge and corner elements, respectively.

The total transmitted field can be viewed as the sum of the embedded fields of all elements in the array, and the embedded fields depend on the mutual coupling [14]. The behavior observed in Fig. 1 motivates an approximate approach where the total field transmitted is constructed from the field distribution of a centrally located element or possibly from a handful of different field distributions corresponding to elements located in the center, on the edge, and at the corners of the array, respectively.

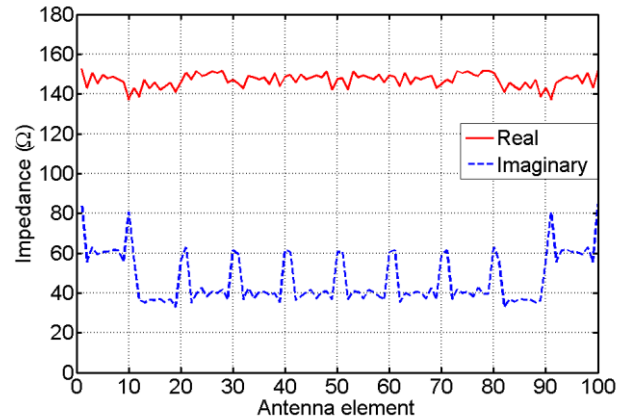


Fig. 1. Impedance characteristics for a uniformly excited 10×10 ground-plane backed dipole array antenna as function of element position. The used inter-element spacing was half a wavelength.

The main idea with the investigated approximate methods is to construct the transmitted field of the array antenna based on embedded assessments of a single or a few elements. In this study, $N \times N$ size arrays were constructed by means of two different methods denoted *Center Element Method* and *Multiple Element Method*, respectively.

Center Element Method: In this method, the transmitted fields of a centrally located element are first determined. The central element is excited in presence of all the other elements terminated in matched loads. In the numerical simulations, the excited element is fed using a transmission line with a characteristic impedance equal to the complex conjugate of the active element impedance with the array scanned towards broadside. With the assumption that the field distribution for most of the elements in large arrays is very similar to the field distribution of a centrally located element, the total field is obtained as the sum of spatially shifted field distributions of the centrally located element. Thus, this approach corresponds to an array with identical embedded fields, thereby neglecting the increasing effects of the array edge for elements located further away from the array center. The field distributions from each identical element are then combined using the Magnitude Method in Eq. (2).

Transmitted fields were approximately constructed for the following cases using the *Center Element Method*:

- With the simulated central element located in an array identical to the array for which the transmitted field was to be constructed. The corresponding results are referred to as *Center Element* results.
- With the simulated central element located in an array of a different size than the array for which the transmitted field was to be constructed. The corresponding results are referred to as *MxM Center Element* results, where *M* denotes the size of the simulated array.

The reason for considering arrays of a different size than the array for which the field is to be constructed is to investigate to what extent the field distributions of smaller arrays may be used to approximate the behavior of a larger array in order to further reduce the computational requirements.

Multiple Element Method: This approach is based on the fact that the characteristics of the array elements differ depending on their location within the array. According to the results presented in Fig. 1, the elements may be grouped into sub-arrays in which the elements experience similar environments as shown in Fig. 2.

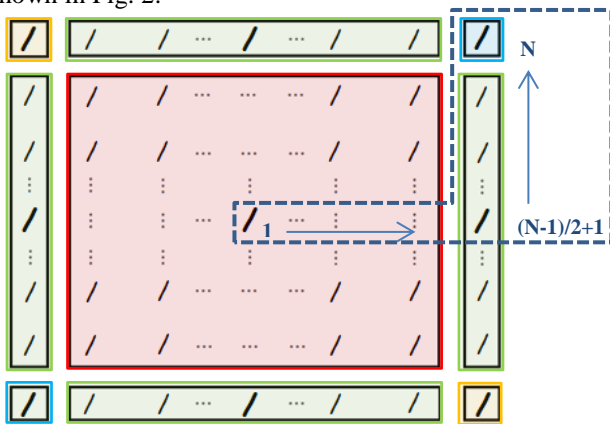


Fig. 2. Schematic illustration of a large array divided into sub-arrays based on the element characteristics. The simulated elements in each sub-array, used to represent the field distribution of all elements in the sub-array, are marked in bold. The numbers 1, $(N-1)/2+1$ and N , corresponds to the element positions used in Fig. 4, and the arrows indicate the directions of increasing element position.

The method considered here is to model $N \times N$ arrays based on combining fields for several different sub-arrays as shown in Fig. 2. Within each sub-array, the field distribution of each element is assumed identical and taken as the field distribution for a corresponding centrally located element (marked in bold in Fig. 2), which here is obtained using an embedded element simulation approach analogous to the approach used for the *Center Element Method*.

Compared with the *Center Element Method*, the *Multiple Element Method* allows for a better representation of the array edge and corner effects, but requires several embedded element simulations instead of one. For the 45° slanted elements considered here and within the approximations of the *Multiple Element Method*, four embedded element simulations are required corresponding to one centre element, one edge element and 2 corner elements. For the subarrays in Fig. 2, one bold element for each colored subarray group needs to be simulated. The field distributions of the other elements within the same subarray group may then be obtained from the simulated field distribution by applying pertinent rotation, mirroring, and translation operations. For simplicity, in this work, 9 different embedded element simulations were made corresponding to the positions of the bold elements in Fig. 2.

Similarly as before, the total transmitted fields are obtained by combining the fields of the spatially distributed elements using the Magnitude Method in Eq. (2).

Transmitted fields were approximately constructed for the following cases:

- With the simulated elements located in the center, on the edge, and at the corners in an array of the same size as the array for which the transmitted field was to be constructed. The corresponding results are referred to as *Multiple Element* results.
- With the simulated elements located in the center, on the edge, and at the corners in an array of a different size than the array for which the transmitted field was to be constructed. The corresponding results are referred to as *MxM Multiple Element* results, where *M* denotes the size of the simulated small array. As a consequence, the 3×3 *Multiple Element Method* is identical to the *Reference Method* for a 3×3 array as in both cases field distributions of the same 9 elements are combined.

Similarly as for the *Center Element Method*, arrays smaller than the array for which the field is to be constructed are considered to investigate to what extent the field distributions of the smaller arrays may be used to approximate the behavior of a larger antenna in order to further reduce the computational requirements.

In Fig. 3, a flow-chart summarizing the steps of the proposed approximate methods for RF EMF compliance assessments of large array antennas is given.

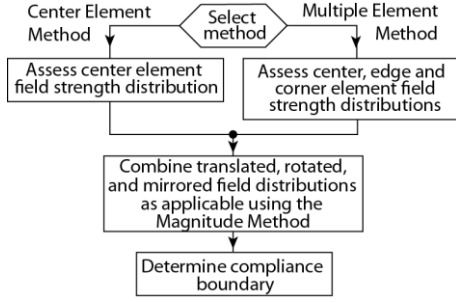


Fig. 3. Flow chart of the proposed approximate methods for RF EMF compliance assessments of large array antennas.

III. RESULTS

In the following section, compliance distance results have been obtained at $f = 2$ GHz for square-shaped arrays ranging from 3×3 to 15×15 elements. The calculated compliance distance, CD , is presented as a function of array size in terms of the relative difference, RD , in percent between the approximate methods and the *Reference Method* according to

$$RD(CD, CD_{\text{ref}}) = \frac{CD - CD_{\text{ref}}}{CD_{\text{ref}}} \times 100 \quad (3)$$

A. Suitability of assumptions as function of array size

To illustrate the suitability of the assumptions behind the approximate methods as function of array size the dipole currents have been determined as function of the element position within the array, see Fig. 4. For each element, the current was determined in magnitude and phase along the length of the dipole. Since the shape of the magnitude and phase curves were found to be very similar for different element positions, the results in Fig. 4 are taken as the values at the center of each element. Element position 1 corresponds to center element of the array whereas element positions $(N-1)/2+1$ and N correspond to edge and corner elements according to Fig. 2. The square-shaped markers indicate the positions of the center, edge and corner elements, respectively, and the circle-shaped markers correspond to the elements located in between.

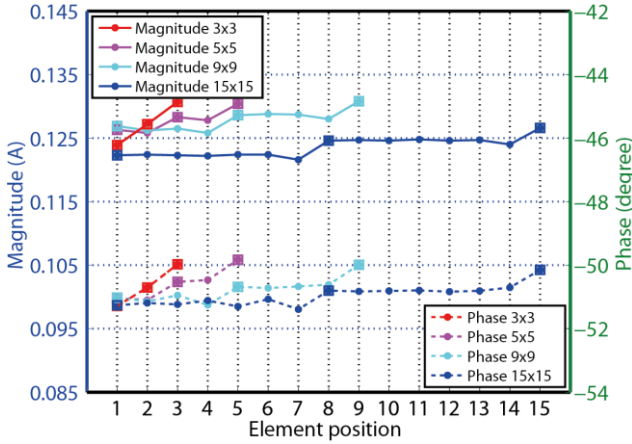


Fig. 4. Magnitude and phase at the center of the dipole elements as function of element position.

In general, the results confirm the assumptions of different behavior for elements located in the center, along the edge, and in the corners of the array with the largest deviations obtained for the smallest arrays. The differences are quite small, however, indicating that the *Center Element Method* may provide quite accurate results also for relatively small arrays.

B. Center and Multiple Element Results

Fig. 5 shows a comparison between the *Center Element* and the *Multiple Element* results with respect to the *Reference Method* in terms of front compliance distance and as function of array size for a total transmitted power of 25 W, 50 W and 75 W, respectively. Very similar results were obtained for the different power levels investigated.

For arrays larger than 3×3 , the relative difference for the *Center Element* method is lower than 4%. As the size increases, the relative difference starts to decrease. For the 15×15 array the relative difference is 1%. Although the results are quite oscillatory in nature, overall a better agreement is observed for the *Multiple Element* results where the edge and corner effects are modeled in a better way. Since the total field strength is given as a summation of several element field strength distributions, the zig-zag behaviour reflects how well the selected element(s) field strength distribution(s) approximates the field strength distributions of the individual elements in the array.

For a transmit power of 25 W, the average absolute relative difference for $N \geq 4$ was found to be 1.1% and 1.6% for the *Center Element Method* and the *Multiple Element Method*, respectively. The rather small numbers obtained confirms the robustness of the proposed approximate methods.

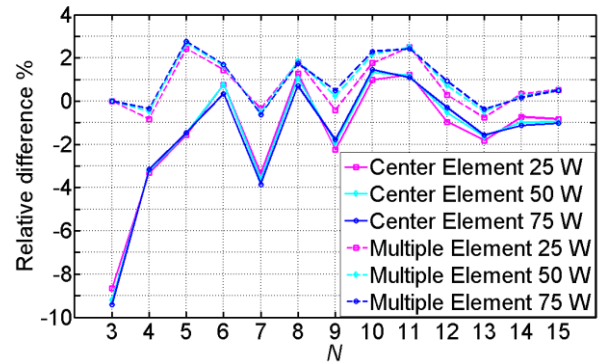


Fig. 5. Relative difference in front compliance distance for the *Center Element* and *Multiple Element* Methods as function of array size.

$M \times M$ *Center Element* and $M \times M$ *Multiple Element* results have been determined for different array sizes transmitting a total power of 25 W. The results are summarized in Table I, also including a comparison with the *Center Element* and *Multiple Element* methods.

TABLE I
RELATIVE DIFFERENCE IN FRONT COMPLIANCE DISTANCE IN PERCENTAGES
FOR VARIOUS CENTER ELEMENT AND MULTIPLE ELEMENT SIMULATION
RESULTS AND ARRAY SIZES WHEN TRANSMITTING A TOTAL POWER OF 25 W.

Methods	Array size for which compliance is assessed		
	7x7	11x11	15x15
Center Element	-3.4	1.2	-0.8
Multiple Element	-0.3	2.5	0.5
3x3 Center Element	-6.3	-5.7	-5.5
5x5 Center Element	-0.4	0.5	1.0
7x7 Center Element	-3.4	-2.8	-2.7
9x9 Center Element	-3.0	-1.7	-1.1
3x3 Multiple Element	-3.3	-3.9	-4.1
5x5 Multiple Element	2.6	2.5	2.5
7x7 Multiple Element	-0.3	-1.1	-1.3
9x9 Multiple Element	0.8	-0.1	-0.2

From the results in Table I, it is clear that the methods based on array sizes different from the array size for which compliance is assessed may result in both less or more accurate results compared with the corresponding *Center Element* and *Multiple Element* solutions. The best overall accuracy was obtained for the *9x9 Multiple Element Method* which provides a very good description of the behavior for the considered arrays.

C. Effects of mutual coupling

As mentioned before, a key requirement to obtain accurate results for investigated type of arrays is that the mutual coupling among the antenna elements is considered. To further study the impact of mutual coupling and to determine the suitability of the proposed methods for various coupling conditions, simulations have been conducted with and without inner metal walls for two different inter-element separation distances (0.5λ and 0.75λ).

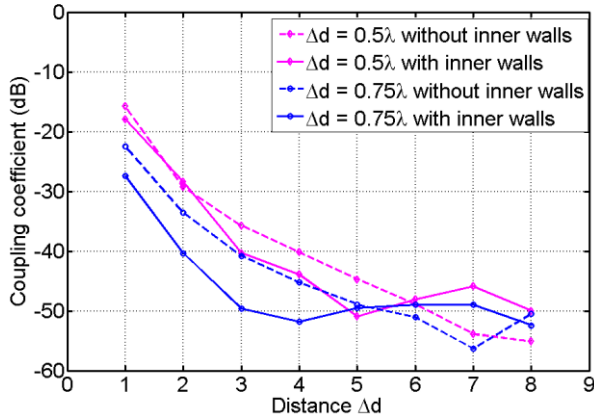


Fig. 6. Coupling coefficient between an active element located at the edge of the center row in a 9x9 array antenna to the other elements in the same row.

In Fig. 6 the mutual coupling magnitude between an active element located at the edge of the center row in a 9x9 array antenna to the other elements in the same row is shown for the considered arrays. The maximum difference in coupling magnitude for the cases considered is in the range 10 to 15 dB

as shown in Fig. 6. As expected, the strongest coupling is in general obtained for the 0.5λ array without walls included.

The front compliance distance was assessed for a 9x9 array antenna with and without inner walls using the *Reference Method*, *Center Element Method* and *5x5 Center Element Method*, respectively. Furthermore, to investigate the effect of different frequencies, the 2 GHz simulations presented above were repeated at 15 GHz. The compliance distance results are given in Table II indicating a very good agreement at both frequencies.

No significant differences are observed for different coupling conditions which confirm the suitability of the proposed methods for different types of array antennas.

TABLE II
COMPARISON OF FRONT COMPLIANCE DISTANCE IN METERS FOR AN ARRAY WITH 9X9 ELEMENTS AS OBTAINED WITH THE REFERENCE, CENTER ELEMENT, AND 5X5 CENTER ELEMENT METHODS (2 GHz / 15 GHz).

Δd	Methods	Transmitted power			
		25 W	50 W	75 W	
With inner walls	0.5λ	Reference	7.4 / 7.4	10.5/10.5	12.9/12.8
		Center Element	7.3/7.3	10.3/10.4	12.6/12.7
		5x5 Center Element	7.4/7.4	10.5/10.5	12.9/12.9
	0.75λ	Reference	10.9/10.9	15.5/15.4	18.9/18.9
		Center Element	11.1/10.9	15.6/15.5	19.0/19.1
		5x5 Center Element	11.1/11.0	15.7/15.6	19.2/19.1
Without inner walls	0.5λ	Reference	7.4/7.3	10.4/10.4	12.7/12.7
		Center Element	7.4/7.4	10.5/10.5	12.9/12.8
		5x5 Center Element	7.7/7.6	10.8/10.8	13.3/13.2
	0.75λ	Reference	10.8/10.8	15.3/15.3	18.7/18.7
		Center Element	10.9/10.9	15.4/15.4	18.9/18.8
		5x5 Center Element	11.0/11.0	15.6/15.5	19.1/19.0

IV. DISCUSSIONS

In this work, the compliance boundary is determined by maximizing the exposure in every evaluation point. This guarantees compliance for all possible array excitations but may be quite conservative when it comes to the actual RF EMF exposure due to the following effects:

- Depending on the radio access specifications, the excitations may have to be selected from a code-book with a finite number of possible antenna weight combinations. This finite number of antenna weights will translate to a finite number of array patterns and a finite number of possible exposure configurations.
- As noted earlier and depending on application and radio conditions, the antenna element excitations are likely to vary over a time frame much shorter than the averaging time prescribed for RF exposure assessments. As the main beam direction is moved accordingly, the average exposure in each direction is reduced compared with the conservative assumption adopted in this work.

A possible remedy is to assess exposure for the different beam-forming states and make use of statistics on the antenna weight selection to determine compliance boundaries which

more reflect the actual exposure conditions. In this context it may also be possible to make use of statistics on realistic maximum power levels, which in several studies have been found to be substantially below the theoretical maximum for different radio access technologies, see e.g. [15, 16].

Although the results in this paper were obtained using numerical simulations based on the Method of Moments (MoM), the approximate methods proposed are general in nature and may be applied also together with full-wave electromagnetic solvers based on other algorithms such as the Finite Element Method (FEM) or the Finite-Difference-Time-Domain Method (FDTD). The approximate methods may also be used for measurements-based compliance assessments.

In the *Center Element Method*, field strength results from a single assessment are used to approximately construct the transmitted field of the array considered. This allows for a significant reduction of the total assessment time. As shown in Table I, quite accurate results were obtained for all cases considered. To study the efficiency of the proposed methods, simulation times and disc storage requirements have been determined and compared with the *Reference Method* for the case of assessing front compliance distance for an array with 15x15 elements. The electric and magnetic field strength levels were assessed on a regular Cartesian grid with a step size of 0.1m in a total volume of 10m³ surrounding the antenna. The following approximate methods were included in the comparison:

- *Center Element Method*
- *Multiple Element Method*
- *5x5 Center Element Method*

The calculations were performed on a HP xw8600 Workstation with 8 core Intel Xeon X 5460 processors and 64 GB of RAM with a clock speed of 3.17 GHz. The comparison results are given in Table III.

TABLE III
COMPUTATIONAL REQUIREMENTS TO DETERMINE FRONT COMPLIANCE
DISTANCE FOR AN ARRAY WITH 15X15 ELEMENTS.

Methods	# of basis functions	Mesh time (min)	Simulation time (h)	Disc storage requirements (GB)
<i>Center Element</i>	30658	18	9.3	0.35
<i>Multiple Element¹</i>	30658	18	83.7	3.2
<i>5x5 Center Element</i>	3563	0.3	0.2	0.35
<i>Reference</i>	30658	18	2092.5	78

The number of antenna elements is 9 times larger for the 15x15 array compared with the 5x5 array, resulting in an almost nine-fold increase in the number of MoM basis functions. The simulation time required to assess EMF exposure from a 15x15 array antenna using the *Reference Method* is approximately 87 days. The *Reference Method* requires 225 separate simulations and consumes 78 GB of memory. By using one of the approximate methods discussed

¹ If the full symmetry properties described in Section II.D had been exploited, the simulation time and disc storage requirements for the Multiple Element Method could have been reduced with a factor of 2.25.

earlier significant savings in computational resources are possible without compromising accuracy.

In order to assess the 15x15 array, the time required to simulate nine elements of the 15x15 array is approximately 3.5 days. The corresponding relative difference in terms of front compliance distance compared with the *Reference Method* was 0.5%. Similarly, the *Center Element Method* and the *5x5 Center Element Method*, requiring a total simulation time of about 9 hours and 0.2 hours, resulted in a relative difference in front compliance distance of 0.8% and 1%, respectively.

V. CONCLUSIONS

In this paper, various approximate methods for RF EMF compliance assessments of RBS products utilizing large array antennas with beam-forming capabilities have been investigated. The results based on field strength assessments for a single or a few elements have been compared with reference results obtained by summing embedded element field strength distributions for all elements within the considered arrays.

It is essential to characterize mutual coupling among the array elements to obtain accurate compliance assessment results. For electrically large arrays, the results also show that accurate compliance boundary dimensions may be obtained using a field-combining procedure of simulation results for a centrally placed element. The *Center Element Method* is attractive since it requires only a single simulation regardless of the number of antenna elements/ports. Compared with the *Reference Method* it provides a significant improvement in simulation time directly proportional to number of elements in the array with a relative error in front compliance distance of a few percent or better.

In general, however, all approximate methods with mutual coupling effects included resulted in a relatively small relative error magnitude. In most cases the relative error stayed below 5% which is to be regarded as a relatively small discrepancy compared with the overall uncertainty in the numerical RF exposure simulations which in many cases may reach levels of 30% or more [17].

REFERENCES

- [1] E. Dahlman, G. Mildh, S. Parkvall, J. Peisa, J. Sachs, and Y. Selen, "5G radio access," *Ericsson Review*, vol. 91, no. 2014-1, pp. 42–47, Jun. 2014.
- [2] J. G. Andrews, S. Buzzi, W. Choi, S. V. Hanly, A. Lozano, A. C. K. Soong, and J. Zhang, "What will 5G be?" *IEEE Journal on Selected Areas in Communications*, vol. 32, no. 6, pp. 1065–1082, Jun. 2014.
- [3] F. W. Vook, A. Ghosh, and T. A. Thomas, "MIMO and beam-forming solutions for 5G technology," in *Microwave Symposium (IMS), 2014 IEEE MTT-S International*, pp. 1–4, Jun. 2014.
- [4] E. Larsson, O. Edfors, F. Tufvesson, and T. Marzetta, "Massive MIMO for next generation wireless systems," *IEEE Communications Magazine*, vol. 52, no. 2, pp. 186–195, Feb. 2014.

- [5] ICNIRP, “Guidelines for limiting exposure to time-varying electric, magnetic, and electromagnetic fields (up to 300 GHz),” *Health Physics*, vol. 74, pp. 494–522, 1998.
- [6] *Basic standard for the calculation and measurement of electromagnetic field strength and SAR related to human exposure from radio base stations and fixed terminal stations for wireless telecommunication systems (110 MHz – 40 GHz)*, CENELEC EN 50383, Aug. 2010.
- [7] A. Faraone, H. Heinrich, T. Harrington, J. Keshvari, T. Onishi, J.-K. Pack, J. Pledl, J. Prats, M. Wood, and P. Zollman, “Guidance for evaluating exposure from multiple EM sources,” IEC, Tech. Rep. TR 62630, 2010.
- [8] N. Perentos, S. Iskra, A. Faraone, R. McKenzie, G. Bit-Babik, and V. Anderson, “Exposure compliance methodologies for multiple input multiple output (MIMO) enabled networks and terminals,” *IEEE Trans. Antennas Propagat.*, vol. 60, no. 2, pp. 644–653, Feb. 2012.
- [9] B. Thors, A. Thielens, J. Fridén, D. Colombi, C. Törnevik, G. Vermeeren, L. Martens, and W. Joseph, “Radio frequency electromagnetic field compliance assessment of multi-band and MIMO equipped radio base stations,” *Bioelectromagnetics*, vol. 35(4), pp. 296–308, Feb. 2014.
- [10] D. F. Kelley, “Embedded element patterns and mutual impedance matrices in the terminated phased array environment,” *Proc. IEEE Antennas and Propagation Society International Symposium, Washington, DC*, vol. 3A, pp. 659–662, Jul. 2005.
- [11] A. Bhattacharyya, *Phased array antennas: Floquet analysis, Synthesis, BFNs, and active array systems*. Wiley-Interscience, 2006.
- [12] E. Dahlman, S. Parkvall, J. S. Parkvall, and J. Skold, *4G: LTE/LTE-Advanced for Mobile Broadband*, 2nd ed. Academic Press, 2011.
- [13] Altair Engineering GmbH, *FEKO User’s Manual*, May 2014.
- [14] R. J. Mailloux, *Phased Array Antenna Handbook*, 2nd ed., ser. Antennas and Propagation Library. Artech House, 2005.
- [15] Z. Mahfouz, A. Gati, D. Lautru, M. F. Wong, J. Wiart, and V. F. Hanna, “Influence of traffic variations on exposure to wireless signals in realistic environments,” *Bioelectromagnetics*, vol. 33(4), pp. 288–297, May 2012.
- [16] D. Colombi, B. Thors, N. Wirén, L.-E. Larsson, and C. Törnevik, “Measurements of downlink power level distributions in LTE networks,” in *Electromagnetics in Advanced Applications (ICEAA), International Conference*, Sep. 2013.
- [17] A. Thielens, G. Vermeeren, D. Kurup, W. Joseph, and L. Martens, “Compliance boundaries for multiple-frequency base station antennas in three directions,” *Bioelectromagnetics*, vol. 34(6), pp. 465–78, Jan. 2013.